

## MIT Open Access Articles

*Electromagnetic Casimir energy of a disk opposite a plane*

The MIT Faculty has made this article openly available. **Please share** how this access benefits you. Your story matters.

**Citation:** Emig, Thorsten, and Noah Graham. "Electromagnetic Casimir Energy of a Disk Opposite a Plane." *Physical Review A* 94.3 (2016): n. pag. © 2016 American Physical Society

**As Published:** <http://dx.doi.org/10.1103/PhysRevA.94.032509>

**Publisher:** American Physical Society

**Persistent URL:** <http://hdl.handle.net/1721.1/105157>

**Version:** Final published version: final published article, as it appeared in a journal, conference proceedings, or other formally published context

**Terms of Use:** Article is made available in accordance with the publisher's policy and may be subject to US copyright law. Please refer to the publisher's site for terms of use.



# Electromagnetic Casimir energy of a disk opposite a plane

Thorsten Emig<sup>1,2,3,\*</sup> and Noah Graham<sup>4,†</sup>

<sup>1</sup>*Laboratoire de Physique Théorique et Modèles Statistiques, CNRS UMR 8626, Bât. 100, Université Paris-Sud, 91405 Orsay Cedex, France*

<sup>2</sup>*Massachusetts Institute of Technology, MultiScale Materials Science for Energy and Environment, Joint MIT-CNRS Laboratory (UMI 3466), Cambridge, Massachusetts 02139, USA*

<sup>3</sup>*Massachusetts Institute of Technology, Department of Physics, Cambridge, Massachusetts 02139, USA*

<sup>4</sup>*Department of Physics, Middlebury College, Middlebury, Vermont 05753, USA*

(Received 5 June 2016; published 15 September 2016)

Building on work by J. Meixner [Z. Naturforschung **3a**, 506 (1948)], we show how to compute the exact scattering amplitude (or T-matrix) for electromagnetic scattering from a perfectly conducting disk. This calculation is a rare example of a nondiagonal T-matrix that can nonetheless be obtained in a semianalytic form. We then use this result to compute the electromagnetic Casimir interaction energy for a disk opposite a plane, for arbitrary orientation angle of the disk, for separations greater than the disk radius. We find that the proximity force approximation (PFA) significantly overestimates the Casimir energy, in the case of both the ordinary PFA, which applies when the disk is parallel to the plane, and the “edge PFA”, which applies when the disk is perpendicular to the plane.

DOI: [10.1103/PhysRevA.94.032509](https://doi.org/10.1103/PhysRevA.94.032509)

## I. INTRODUCTION

Scattering methods have greatly expanded the range of situations in which one can compute the Casimir energy [1] of quantum electrodynamics. In this approach, one decomposes the path integral representation of the Casimir energy [2] as a log-determinant [3] in terms of a multiple scattering expansion, as was done for asymptotic separations in Refs. [4] and [5]. This representation is closely connected to the Krein formula [6–8] relating the density of states to the scattering matrix for an ensemble of objects. It can also be regarded as a concrete implementation of the perspective emphasized by Schwinger [9] that the fluctuations of the electromagnetic field can be traced back to charge and current fluctuations on the objects.

The scattering method was first developed for general shapes in the context of van der Waals interactions [10]. In planar geometries, the scattering approach yields the Casimir energy in terms of reflection coefficients [11–13]. By relating the scattering matrix for a collection of spheres [14] or disks [15] to the objects’ individual scattering matrices, Bulgac, Magierski, and Wirzba were also able to use this result to investigate the scalar and fermionic Casimir effect for disks and spheres [16–18]. A more general formalism, developed in [19–21], has made it possible to extend these results to other coordinate systems, an approach that is particularly useful for geometries, such as the ones we consider here, with edges and tips [22–30]. It can also be applied to dilute objects in perturbation theory [31] and extended to efficient, general-purpose numerical calculations [32]; a review and further references can be found in Ref. [33]. In this approach, each object is characterized by its scattering amplitude, also known as the T-matrix, which describes its response to an electromagnetic fluctuation. It can therefore be implemented for any object whose T-matrix can be calculated using a basis for which an expansion of the free electromagnetic Green’s function exists [34].

For scalar models, the Casimir energy of a disk opposite a plane has been calculated for a general angle between the disk axis and the normal to the plane [35] as the zero-radius limit of an oblate spheroid. Unfortunately, for electromagnetism the wave equation in spheroidal coordinates is not separable. However, Meixner [36] has developed a calculation of diffraction for a disk, using a spheroidal vector basis. By extending this calculation, including an additional subtlety of the case where the azimuthal quantum number  $m$  is 0, we obtain the T-matrix in this basis and use it to calculate the Casimir energy for a perfectly conducting disk opposite a plane. This T-matrix is nondiagonal, and the basis in which it is expressed is not orthonormal. Nonetheless, we can implement appropriate conversions to make it amenable to the calculation of the Casimir interaction energy. We apply this method to the case of a disk opposite a plane, including rotations of the disk axis relative to the normal to the plane. This calculation enables us to extend results for conductors with edges in Casimir systems to an example involving a compact object.

## II. THE T-MATRIX

In this section, we calculate the T-matrix for an infinitely thin and perfectly conducting disk. Here, we build on an earlier calculation for this scattering problem, done by Meixner in his classic paper [36].<sup>1</sup> However, as we see, that solution was incomplete; we extend it to obtain the full T-matrix, as required for Casimir calculations.

### A. Electromagnetic scattering from an infinitely thin conducting disk

We consider a perfectly conducting, infinitely thin disk of radius  $R$  lying in the  $z = 0$  plane, with the  $z$  axis being the symmetry axis of the disk. This idealized case models

\*emig@mit.edu

†ngraham@middlebury.edu

<sup>1</sup>An English translation due to N. Sadeh is available from the authors.

thin disks, where the thickness of the disk is assumed to be small compared to the wavelength of the electromagnetic field but large enough for the disk to be perfectly reflecting at the wavelengths of interest. We consider the case of zero temperature, although it is straightforward to extend our calculation to include thermal effects as well.

For a given incoming electric field  $\mathbf{E}^{\text{in}}$ , we find the corresponding outgoing wave  $\mathbf{E}^{\text{out}}$  such that the boundary conditions on the disk are satisfied. The standard boundary conditions require that the tangential component of the electric field  $(\mathbf{E}^{\text{in}} + \mathbf{E}^{\text{out}})_{\text{tang}}$  vanishes on the disk. Were the disk a smooth body without its sharp edge, this condition would be enough to solve the physical scattering problem. However, the sharpness of the infinitely thin disk causes the outgoing field to diverge on the edge. It turns out that there are many outgoing solutions that satisfy the boundary conditions but diverge at the edge in a way such that the integrated electromagnetic energy density is infinite [36]. Such outgoing solutions are nonphysical mathematical solutions of the scattering problem. There is only one solution that diverges slowly enough so that the electromagnetic energy density when integrated is still finite. As a result, this edge condition uniquely fixes the physically correct scattering solution.

The physical scattering problem for an infinitely thin disk can then be formulated in the following way:

- (1) The fields  $(\mathbf{E}^{\text{in}}, \mathbf{E}^{\text{out}})_{\text{tang}}$  obey the Maxwell equations.
- (2) At large distances, the outgoing wave behaves like an outgoing spherical wave with an angular-dependent amplitude.
- (3) On the disk the field satisfies the boundary conditions  $(\mathbf{E}^{\text{in}} + \mathbf{E}^{\text{out}})_{\text{tang}} = 0$ .
- (4) On the edge, the field satisfies the edge condition, i.e., the field diverges slowly enough that the electromagnetic energy of the outgoing field is finite.

Note that the edge condition involves the outgoing field only, because the incoming field does not diverge on the edge. Of course, the scattering problem can equivalently be formulated in terms of the magnetic field  $\mathbf{B}$ .

### 1. The Debye potentials

In the following, we use natural units where  $c = \mu_0 = \varepsilon_0 = 1$ . Following Meixner [36], we express the  $\mathbf{E}$  and  $\mathbf{B}$  fields in terms of the scalar Debye potentials  $\Pi_1$  and  $\Pi_2$ ,

$$\mathbf{E} = \nabla \times \nabla \times (\mathbf{r} \Pi_1) + i k \nabla \times (\mathbf{r} \Pi_2), \quad (1)$$

$$\mathbf{B} = -i k \nabla \times (\mathbf{r} \Pi_1) + \nabla \times \nabla \times (\mathbf{r} \Pi_2). \quad (2)$$

Here,  $k$  is the wave number and  $\mathbf{r}$  is the position vector  $\mathbf{r} = (x, y, z)$ . The Debye potentials solve the scalar wave equation

$$\Delta \Pi_i + k^2 \Pi_i = 0 \quad \text{for } i = 1, 2, \quad (3)$$

and therefore the  $\mathbf{E}$  and  $\mathbf{B}$  fields obey the Maxwell equations

$$\nabla \times \mathbf{E} = i k \mathbf{B}, \quad \nabla \times \mathbf{B} = -i k \mathbf{E}. \quad (4)$$

To express the boundary conditions for the electric field in terms of the Debye potentials, it is useful to switch to cylindrical coordinates  $(\rho, \varphi, z)$ . Due to the axial symmetry of the problem, it is sufficient to consider Debye potentials of the form  $\Pi_{1,2}(\rho, \varphi, z) = \Pi_{1,2}(\rho, z) e^{i m \varphi}$ , where  $m$  is the conserved azimuthal quantum number. Since the incoming and the

outgoing fields have the same  $\varphi$  dependence, this dependence can be expressed as a Fourier series and considered term by term. Let us therefore substitute  $\Pi_{1,2}(\rho, \varphi, z) = \Pi_{1,2}(\rho, z) e^{i m \varphi}$  into Eq. (1). To eliminate the second derivative with respect to  $z$ , we use Eq. (3). Then, dropping the common factor of  $e^{i m \varphi}$ , the  $\rho$  and  $\varphi$  components of the electric field  $\mathbf{E}$  become

$$E_\rho = k^2 \rho \Pi_1(\rho, 0) + 2 \partial_\rho \Pi_1(\rho, 0) + \rho \partial_\rho^2 \Pi_1(\rho, 0), \quad (5)$$

$$E_\varphi = i \frac{m \Pi_1(\rho, 0)}{\rho} + k \rho \partial_z \Pi_2(\rho, 0) + m \partial_\rho \Pi_1(\rho, 0). \quad (6)$$

Both  $E_\rho$  and  $E_\varphi$  have to vanish on the disk. We first solve Eq. (5) for  $\Pi_1(\rho, 0)$  and then Eq. (6) for  $\partial_z \Pi_2(\rho, 0)$  and get

$$\rho \Pi_1(\rho, 0) = \alpha \cos(k \rho) + \beta \sin(k \rho), \quad (7)$$

$$\rho^2 \partial_z \Pi_2(\rho, 0) = m (\alpha \sin(k \rho) - \beta \cos(k \rho)). \quad (8)$$

Equations (7) and (8) represent the boundary conditions expressed in terms of the Debye potentials. The functions  $\alpha$  and  $\beta$  depend on  $k$  and  $m$ . The boundary conditions are trivially satisfied if  $\alpha = \beta = 0$ . Yet even the trivial solution may violate the edge conditions if the incoming wave is not 0. In general, the physical solution is built out of the trivial solution plus a special solution with nonzero  $\alpha$  and  $\beta$  by exploiting the edge conditions.

Note that if  $m = 0$ , the right-hand side of Eq. (8) vanishes identically. This case was not considered by Meixner in [36]. One must consider this case more carefully to avoid a free undetermined parameter in the equations or to a situation where the edge condition cannot be satisfied at all, resulting in an unphysical solution. We consider this case later, but first we formulate the edge conditions.

### 2. The edge conditions

Let us now use coordinates appropriate for the scattering problem. The infinitely thin disk can be considered as a limiting case of an oblate spheroid, so that in the following we will use oblate spheroidal coordinates  $(\xi, \eta, \varphi)$ . They are related to the Cartesian coordinates via

$$x = R \sqrt{(1 + \xi^2)(1 - \eta^2)} \cos(\varphi), \quad (9)$$

$$y = R \sqrt{(1 + \xi^2)(1 - \eta^2)} \sin(\varphi), \quad (10)$$

$$z = R \xi \eta, \quad (11)$$

where

$$0 \leq \xi < \infty, \quad -1 \leq \eta \leq 1, \quad 0 \leq \varphi \leq 2\pi. \quad (12)$$

The  $\xi = 0$  surface is then just the disk in the  $z = 0$  plane having radius  $R$  and the  $z$  axis as a symmetry axis. The center of the disk corresponds to  $(\xi = 0, \eta = \pm 1)$  and the edge is described by  $(\xi = 0, \eta = 0)$ . We assume that the Debye potentials can be expanded in a Taylor series in terms of  $\xi$  and  $\eta$  on the edge. The edge conditions, which guarantee that the integrated energy density stays finite, read [36]

$$\frac{\partial \Pi_1}{\partial \xi} = \frac{\partial \Pi_1}{\partial \eta} = \frac{\partial \Pi_2}{\partial \xi} = \frac{\partial \Pi_2}{\partial \eta} = 0 \quad \text{for } \xi = \eta = 0. \quad (13)$$

To derive Eq. (13), we have to express  $\Pi_1$  and  $\Pi_2$  as a power series in  $\xi$  and  $\eta$ , calculate the electromagnetic field using Eqs. (1) and (2), and then integrate the electromagnetic energy density. Then the divergences can be ruled out by imposing Eq. (13).

Let us decompose the Debye potentials into incoming and outgoing parts,

$$\Pi_i = \Pi_i^{\text{in}} + \Pi_i^{\text{out}} + \overline{\Pi}_i^{\text{out}}, \quad i = 1, 2. \quad (14)$$

Here, it is useful to set  $\Pi_i^{\text{out}} = \overline{\Pi}_i^{\text{out}} + \overline{\overline{\Pi}}_i^{\text{out}}$ ,  $i = 1, 2$ . For  $\overline{\Pi}_i^{\text{out}}$  on the disk we require

$$\Pi_1^{\text{in}} + \overline{\Pi}_1^{\text{out}} \equiv 0, \quad \frac{\partial}{\partial z}(\Pi_2^{\text{in}} + \overline{\Pi}_2^{\text{out}}) \equiv 0 \quad \text{for} \quad \xi = 0. \quad (15)$$

The sum  $\Pi_i^{\text{in}} + \overline{\Pi}_i^{\text{out}}$  represents the trivial solution in Eqs. (7) and (8). The second part of the outgoing Debye potential is then the special solution of the same Eqs. (7) and (8). Note that since the incoming wave fulfills the edge conditions, instead of Eq. (13) it is sufficient to require

$$\frac{\partial \Pi_1^{\text{out}}}{\partial \xi} = \frac{\partial \Pi_1^{\text{out}}}{\partial \eta} = \frac{\partial \Pi_2^{\text{out}}}{\partial \xi} = \frac{\partial \Pi_2^{\text{out}}}{\partial \eta} = 0 \quad (16)$$

for  $\xi = \eta = 0$ . In the following sections we derive the solution for  $\Pi_i^{\text{in, out}}$ ,  $\overline{\Pi}_i^{\text{out}}$ , and  $\overline{\overline{\Pi}}_i^{\text{out}}$  in terms of spheroidal functions.

### 3. Debye potentials in terms of spheroidal functions

There are several coordinate systems in which Eq. (3) can be separated. For example, in spherical coordinates, every solution of Eq. (3) can be expanded in terms of spherical waves  $h_n(kr)P_n^m(\cos\theta)\exp(im\varphi)$ , where  $(r, \theta, \varphi)$  are the spherical coordinates,  $n$  and  $m$  are spherical quantum numbers,  $P_n^m$  are the Legendre polynomials, and  $h_n$  are the (incoming or outgoing) spherical Hankel functions. The separation of the wave equation can also be done in spheroidal coordinates  $(\xi, \eta, \phi)$ . The equivalents of the spherical radial and angular function then are the radial and angular spheroidal functions. The spheroidal wave functions  $L$  are called *Lamé* functions and are written as [37,38]

$$L_{n,m}^{(1)}(\xi, \eta, \varphi; i\gamma) = S_{n,m}^{(1)}(-i\xi; i\gamma)Sp_{n,m}(\eta; i\gamma)e^{im\varphi}, \quad (17)$$

$$L_{n,m}^{(3)}(\xi, \eta, \varphi; i\gamma) = S_{n,m}^{(3)}(-i\xi; i\gamma)Sp_{n,m}(\eta; i\gamma)e^{im\varphi}, \quad (18)$$

where the first function represents the incoming wave and the second function the outgoing wave. In contrast to their spherical equivalents, the radial and angular spheroidal functions,  $S$  and  $Sp$ , depend on  $\gamma \equiv kR$ . In addition, the radial spheroidal function also depends on  $m$ . Both the angular and the radial spheroidal functions become their spherical equivalents as  $\gamma \rightarrow 0$  and  $\xi \rightarrow \infty$ , and spherical waves can be expanded in terms of spheroidal waves, and vice versa. The factors of  $\pm i$  in the arguments to the spheroidal functions correspond to the oblate case. Finally, we note that, analogously to the spherical case,  $S_{n,m}^{(1)}(0; i\gamma) = Sp_{n,m}(0; i\gamma) = 0$  for  $n - m$  even and  $\partial_\xi S_{n,m}^{(1)}(0; i\gamma) = \partial_\eta Sp_{n,m}(\eta = 0; i\gamma) = 0$  for  $n - m$  odd. In addition,  $Sp_{n,m}(\eta; i\gamma)$  is even (odd) in  $\eta$  for  $n - m$  even (odd).

### 4. The first part of the scattered field $\overline{\Pi}_i^{\text{out}}$

Having chosen the appropriate wave basis, let us return to the scattering problem. Since the Maxwell equations, (1), are linear in  $\Pi_1$  and  $\Pi_2$ , it is sufficient to restrict ourselves to the two cases

$$\Pi_1^{\text{in}} = L_{n_0, m_0}^{(1)}, \quad \Pi_2^{\text{in}} = 0 \quad (19)$$

and

$$\Pi_1^{\text{in}} = 0, \quad \Pi_2^{\text{in}} = L_{n_0, m_0}^{(1)} \quad (20)$$

for some  $n_0, m_0$ . In this regard we do not consider incoming plane waves as Meixner in [36] but, instead, work in a basis of vector spheroidal functions.

The first part,  $\overline{\Pi}_i^{\text{out}}$ , of the decomposed outgoing potential,  $\Pi_i^{\text{out}} = \overline{\Pi}_i^{\text{out}} + \overline{\overline{\Pi}}_i^{\text{out}}$  ( $i = 1, 2$ ), can then be found straightforwardly. Considering the first case,  $\Pi_1^{\text{in}} = L_{n_0, m_0}^{(1)}$ ,  $\Pi_2^{\text{in}} = 0$ , one obtains

$$\overline{\Pi}_1^{\text{out}} = -L_{n_0}^{m_0(3)}(\xi, \eta, \varphi; i\gamma) \frac{S_{n_0}^{m_0(1)}(-i0, i\gamma)}{S_{n_0}^{m_0(3)}(-i0, i\gamma)}, \quad \overline{\Pi}_2^{\text{out}} = 0. \quad (21)$$

For the second case,  $\Pi_1^{\text{in}} = 0$ ,  $\Pi_2^{\text{in}} = L_{n_0, m_0}^{(1)}$ , the analogous calculation shows that

$$\overline{\Pi}_1^{\text{out}} = 0, \quad \overline{\Pi}_2^{\text{out}} = -L_{n_0}^{m_0(3)}(\xi, \eta, \varphi; i\gamma) \frac{S_{n_0}^{m_0(1)}(-i0, i\gamma)}{S_{n_0}^{m_0(3)}(-i0, i\gamma)}. \quad (22)$$

The derivative in Eq. (22) is taken with respect to  $\xi$ . To derive Eqs. (21) and (22), we used Eq. (15).

In general, the edge conditions in Eq. (13) will be violated if we substitute in Eq. (13) the first part  $\overline{\Pi}_i^{\text{out}}$  only. The second part  $\overline{\overline{\Pi}}_i^{\text{out}}$  is needed to match the edge conditions. However, for some values of  $n_0$  and  $m_0$ , the boundary conditions are satisfied by the incoming field alone and the outgoing field vanishes identically. Since  $S_{n_0}^{m_0(1)}(-i0, i\gamma) \equiv 0$  for  $n_0 - m_0$  odd, and  $S_{n_0}^{m_0(1)}(-i0, i\gamma) \equiv 0$  for  $n_0 - m_0$  even, there is no scattered field for  $n_0 - m_0$  odd in the first case and  $n_0 - m_0$  even in the second. In the next section we construct  $\overline{\overline{\Pi}}_i^{\text{out}}$  for general  $n_0$  and  $m_0$ .

### 5. The second part of the scattered field $\overline{\overline{\Pi}}_i^{\text{out}}$

The second part of the scattered Debye potential  $\overline{\overline{\Pi}}_j^{\text{sc}}$  can be expanded in terms of outgoing waves,

$$\overline{\overline{\Pi}}_1^{\text{out}} = \sum_{n=|m_0|}^{\infty} A_n^{n_0, m_0} L_n^{m_0(3)}(\xi, \eta, \varphi, i\gamma), \quad (23)$$

$$\overline{\overline{\Pi}}_2^{\text{out}} = \sum_{n=|m_0|}^{\infty} B_n^{n_0, m_0} L_n^{m_0(3)}(\xi, \eta, \varphi, i\gamma). \quad (24)$$

To get the functions  $A_n^{n_0, m_0}$  and  $B_n^{n_0, m_0}$ , Eqs. (23) and (24) are substituted into Eqs. (7) and (8). Using the orthogonality of the  $Sp$  functions with the normalization convention as in *Mathematica* and Meixner-Schaefer [37],

$$\int_{-1}^1 Sp_n^m(\eta) Sp_l^m(\eta) d\eta = \frac{2(n+m)!}{(2n+1)(n-m)!} \delta_{nl}, \quad (25)$$

and recalling that  $\rho^2 = R^2(1 - \eta^2)$ , we can project the expressions onto the  $Sp$  functions, thus eliminating the infinite sums. Then  $A_n^{n_0, m_0}$  and  $B_n^{n_0, m_0}$  can be expressed in terms of  $\alpha$  and  $\beta$  as

$$A_n^{n_0, m_0} = \alpha^{n_0, m_0} a_1^{n, m_0} + \beta^{n_0, m_0} b_1^{n, m_0}, \quad (26)$$

$$B_n^{n_0, m_0} = \alpha^{n_0, m_0} a_2^{n, m_0} + \beta^{n_0, m_0} b_2^{n, m_0}. \quad (27)$$

Here we have explicitly included the  $n_0, m_0$  indices on  $\alpha$  and  $\beta$ . In addition, we introduced new functions  $a_1, b_1, a_2, b_2$  as

$$a_1^{n, m_0} = \frac{N_{n, m_0}}{S_n^{m_0(3)}(-i0)} \int_{-1}^1 Sp_n^{m_0}(\eta) \frac{\cos(\gamma \sqrt{1 - \eta^2})}{R \sqrt{1 - \eta^2}} d\eta, \quad (28)$$

$$b_1^{n, m_0} = \frac{N_{n, m_0}}{S_n^{m_0(3)}(-i0)} \int_{-1}^1 Sp_n^{m_0}(\eta) \frac{\sin(\gamma \sqrt{1 - \eta^2})}{R \sqrt{1 - \eta^2}} d\eta, \quad (29)$$

$$a_2^{n, m_0} = \frac{m_0 N_{n, m_0}}{S_n^{m_0(3)}(-i0)} \int_{-1}^1 Sp_n^{m_0}(\eta) \eta \frac{\sin(\gamma \sqrt{1 - \eta^2})}{1 - \eta^2} d\eta, \quad (30)$$

$$b_2^{n, m_0} = \frac{-m_0 N_{n, m_0}}{S_n^{m_0(3)}(-i0)} \int_{-1}^1 Sp_n^{m_0}(\eta) \eta \frac{\cos(\gamma \sqrt{1 - \eta^2})}{1 - \eta^2} d\eta, \quad (31)$$

with

$$N_{n, m} = \frac{(2n + 1)(n - m)!}{2(n + m)!}. \quad (32)$$

Note that apart from their indices, the functions  $A, B, \alpha, \beta, a_1, b_1, a_2$ , and  $b_2$  depend on  $\gamma$ , and in Eqs. (28)–(30) we have also suppressed the dependence on  $\gamma$  in the functions  $S$  and  $Sp$ . Note also that  $a_1^{n, m_0}, b_1^{n, m_0}$  vanish for  $n - m_0$  odd, and  $a_2^{n, m_0}, b_2^{n, m_0}$  vanish for  $n - m_0$  even. Indeed for  $n - m_0$  odd, the function  $Sp_n^{m_0}(\eta)$  is odd in  $\eta$ . Since it is multiplied by an even function in  $\eta$  in Eq. (28) and (29), the integrals for  $a_1$  and  $b_1$  vanish. Analogously, one verifies the second case.

So far, we have strictly followed Meixner [36], implicitly assuming  $m_0 \neq 0$ . For  $m_0 = 0$ , the functions  $a_2$  vanishes identically, whereas the function  $b_2$  becomes ill defined: on the one hand, the integral in Eq. (31) is multiplied by  $m_0 = 0$ , and on the other hand, the integral itself diverges. The case  $m_0 = 0$  therefore requires further consideration. For  $m_0 = 0$ , Eq. (8) simply reads  $\rho \partial_z \Pi_2 = 0$ , meaning that  $\Pi_2$  is proportional to a  $\delta$  function of  $\rho$ . As a result, we find  $a_2^{n, 0} = 0$  and  $b_2^{n, 0} = -(2n + 1)[Sp_n^0(1) - Sp_n^0(-1)]/2S_n^{m_0(3)}(-i0)$ , where we write the right-hand side of Eq. (27) as  $\tilde{\beta}^{n_0, 0} b_2^{n, 0}$  for the case of  $m_0 = 0$ .

## 6. Calculation of $\alpha^{n_0, m_0}$ and $\beta^{n_0, m_0}$

In this section we calculate the functions  $\alpha^{n_0, m_0}$  and  $\beta^{n_0, m_0}$  of Eqs. (26) and (27). Then we will be able to determine the second part of the scattered Debye potential,  $\bar{\Pi}_1^{\text{sc}}$ , which, together with the known first part, Eqs. (21) and (22), will eventually lead to the scattered field. For  $m_0 \neq 0$ , there are two unknown functions,  $\alpha^{n_0, m_0}$  and  $\beta^{n_0, m_0}$ , which can be calculated from the edge conditions in Eq. (16). There are four edge conditions, but it turns out that that two of them, the second and third of Eq. (16), are always fulfilled, whereas the first and

the fourth yield the two equations needed to determine  $\alpha^{n_0, m_0}$  and  $\beta^{n_0, m_0}$ .

For  $m_0 = 0$ , as we mentioned at the end of the last section, there are three functions,  $\alpha^{n_0, m_0}, \beta^{n_0, m_0}$  and  $\tilde{\beta}^{n_0, 0}$ , that need to be determined. At first glance, the system of three unknowns and only two equations seems to be overdetermined. But as we will see, it is necessary to set  $\alpha^{n_0, 0} = 0$ , because otherwise the scattered solution will diverge in the center of the disk.

Let us now consider the following two cases for incoming fields, from which all incoming fields can be constructed.

## 7. The case $\Pi_1^{\text{in}} \neq 0, \Pi_2^{\text{in}} = 0$

Using the fourth edge condition in Eq. (16), we obtain (with  $\bar{\Pi}_2^{\text{out}} = 0$ )

$$\partial_\eta \bar{\Pi}_2^{\text{out}} = 0 \quad \text{for} \quad \xi = \eta = 0, \quad (33)$$

where  $\bar{\Pi}_2^{\text{out}}$  is given by Eq. (24). Expressing  $B_n^{n_0, m_0}$  as in Eq. (27), we get

$$\begin{aligned} \alpha^{n_0, m_0} \sum_{n=|m_0|+1}^{\infty} a_2^{n, m_0}(\gamma) S_n^{m_0(3)}(-i0) Sp_n^{m_0}(0) \\ = -\beta^{n_0, m_0} \sum_{n=|m_0|+1}^{\infty} b_2^{n, m_0}(\gamma) S_n^{m_0(3)}(-i0) Sp_n^{m_0}(0). \end{aligned} \quad (34)$$

The sum starts at  $n = |m_0| + 1$ , since  $Sp_n^{m_0}(\eta = 0) = 0$  for  $n - m_0$  even. For  $m_0 = 0$ , the first series vanishes, since  $a_2^{n, 0} = 0$ , whereas  $\beta^{n_0, 0}$  in Eq. (34) has to be replaced by  $\tilde{\beta}^{n_0, 0}$ . To satisfy the edge condition, we therefore need  $\tilde{\beta}^{n_0, 0} = 0$ , such that  $\bar{\Pi}_2^{\text{sc}}$  vanishes identically.

For  $m_0 \neq 0$ , we can express  $\beta^{n_0, m_0}$  as

$$\beta^{n_0, m_0} = -q_1^{m_0}(\gamma) \alpha^{n_0, m_0}. \quad (35)$$

The function  $q_1^{m_0}(\gamma)$  can be calculated from Eq. (34) as

$$q_1^{m_0}(\gamma) = \frac{sa_2^{m_0}(\gamma)}{sb_2^{m_0}(\gamma)}, \quad (36)$$

where the functions  $sa_2^{m_0}$  and  $sb_2^{m_0}$  have been defined as

$$sa_2^{m_0}(\gamma) = \sum_{n=|m_0|+1}^{\infty} a_2^{n, m_0}(\gamma) S_n^{m_0(3)}(-i0) Sp_n^{m_0}(0) \quad (37)$$

and

$$sb_2^{m_0}(\gamma) = \sum_{n=|m_0|+1}^{\infty} b_2^{n, m_0}(\gamma) S_n^{m_0(3)}(-i0) Sp_n^{m_0}(0). \quad (38)$$

Note that the ratio  $q_1^{m_0}(\gamma)$  does not depend on  $n_0$ .

Unfortunately, the series needed for calculating  $q_1^{m_0}$  do not converge if written as in Eqs. (37) and (38). The reason is that the derivative with respect to  $\eta$  has been put inside the series. However, evaluating the series with  $Sp$  instead of  $Sp'$  we get well-behaved functions of  $\eta$  with a well-defined derivative at  $\eta = 0$ . We remedy this problem by subtracting the leading term in  $\gamma$ , which can then be added back in within an analytic computation. The leading-order integrals necessary for this subtraction can be computed analytically



using Eqs. (A4), (A5), (A6), and (A7), as summarized in the Appendix.

The leading order of  $q_1^{m_0}(\gamma)$  can be found analytically for any  $m_0$ . For small  $\gamma$  and  $m_0 \geq 0$  even we find

$$sa_2^{m_0}(\gamma) = -\frac{\gamma(m_0-1)!!}{(m_0-2)!!} + O(\gamma^3) \quad (39)$$

and

$$sb_2^{m_0}(\gamma) = \frac{2m_0!!}{\pi(m_0-1)!!} + O(\gamma^2), \quad (40)$$

and for  $m_0 > 0$  odd we have

$$sa_2^{m_0}(\gamma) = -\frac{2\gamma(m_0-1)!!}{\pi(m_0-2)!!} + O(\gamma^3) \quad (41)$$

and

$$sb_2^{m_0}(\gamma) = \frac{m_0!!}{(m_0-1)!!} + O(\gamma^2). \quad (42)$$

Subtracting the leading order from the diverging series term by term renders them convergent and numerically evaluable. It is straightforward to extend these results to  $m_0 < 0$ , since both sums are invariant under  $m_0 \rightarrow -m_0$ .

The remaining edge condition,

$$\frac{\partial}{\partial \xi} (\overline{\Pi}_1^{\text{out}} + \overline{\overline{\Pi}}_1^{\text{out}}) = 0 \quad \text{for} \quad \xi = \eta = 0, \quad (43)$$

fixes  $\alpha^{n_0, m_0}$ , which for  $m_0 \neq 0$  can be found from Eqs. (21), (23), (26), and (35):

$$\alpha_1^{n_0, m_0}(\gamma) = \frac{S_{n_0}^{\prime m_0(3)}(-i0)Sp_{n_0}^{m_0}(0)S_{n_0}^{m_0(1)}(-i0)}{[sa_1^{m_0}(\gamma) - q_1^{m_0}sb_1^{m_0}(\gamma)]S_{n_0}^{m_0(3)}(-i0)}. \quad (44)$$

Note the subscript of  $\alpha^{n_0, m_0}$ , which we added for clarity since  $\alpha^{n_0, m_0}$  will have a different functional form in the second case,  $\Pi_1^{\text{in}} = 0, \Pi_2^{\text{in}} \neq 0$ , considered in the next section. Analogously to Eqs. (37) and (38), here  $sa_1^{m_0}$  and  $sb_1^{m_0}$  have been defined as

$$sa_1^{m_0}(\gamma) = \sum_{n=|m_0|}^{\infty} a_1^{n, m_0}(\gamma)S_n^{\prime m_0(3)}(-i0)Sp_n^{m_0}(0) \quad (45)$$

and

$$sb_1^{m_0}(\gamma) = \sum_{n=|m_0|}^{\infty} b_1^{n, m_0}(\gamma)S_n^{\prime m_0(3)}(-i0)Sp_n^{m_0}(0). \quad (46)$$

Once again, the series in Eqs. (45) and (46) only converge if the derivative with respect to  $\xi$  is taken after the summation over  $n$ , so we again subtract the leading behavior at small  $\gamma$ , which is responsible for the divergence. This subtraction can then be added back in as an analytic expression for any  $m_0$ . For small  $\gamma$  and  $m_0 \geq 0$  even we obtain

$$sa_1^{m_0}(\gamma) = -\frac{(m_0-1)!!}{(m_0-2)!!} + O(\gamma^2) \quad (47)$$

and

$$sb_1^{m_0}(\gamma) = -\frac{2m_0!!\gamma}{\pi(m_0-1)!!} + O(\gamma^3), \quad (48)$$

and for  $m_0 > 0$  odd we have

$$sa_1^{m_0}(\gamma) = -\frac{2(m_0-1)!!}{\pi(m_0-2)!!} + O(\gamma^2) \quad (49)$$

and

$$sb_1^{m_0}(\gamma) = -\frac{m_0!!\gamma}{(m_0-1)!!} + O(\gamma^3), \quad (50)$$

while for negative  $m_0$  we use that these sums are odd in  $m_0 \rightarrow -m_0$ .

A special case arises for  $m_0 = 0$ . Equations (26) and (27) decouple, and strictly speaking, we now have to distinguish between  $\alpha, \beta$  in Eq. (26) and  $\alpha, \beta$  in Eq. (27), which are no longer related. Let us consider Eq. (34) for  $m_0 = 0$ . Since  $a_2^{n,0} \equiv 0$ , the left-hand side of Eq. (34) vanishes identically, and so must the right-hand side. Consequently, this implies  $\Pi_2^{\text{out}} = 0$ . Now we are left with two unknowns,  $\alpha$  and  $\beta$ , in Eq. (26). If we keep  $\alpha \neq 0$ , the derivative of the potential  $\Pi_1$  with respect to  $\xi$  will fail to converge for  $\eta = \pm 1$ . This would imply a diverging  $\mathbf{E}_n$  in the center of the disk. This divergence occurs only for  $m_0 = 0$  and can be cured by setting  $\alpha = 0$  in Eq. (26). Remarkably, for  $m_0 > 0$ , the  $Sp$  functions vanish at  $\eta = \pm 1$  and the field stays finite. Thus we also luckily get rid of an overcounted parameter. The first term and the series over  $b_1$  can then be calculated and we find  $\beta^{n_0, m_0=0}$  as a function of  $\gamma$  by exploiting the edge condition in Eq. (43) to obtain

$$\beta_1^{n_0, 0}(\gamma) = \frac{S_{n_0}^{\prime 0(3)}(-i0)Sp_{n_0}^0(0)S_{n_0}^{0(1)}(-i0)}{sb_1^0(\gamma)S_{n_0}^{0(3)}(-i0)}. \quad (51)$$

### 8. The case $\Pi_1^{\text{in}} = 0, \Pi_2^{\text{in}} \neq 0$

The second case,  $\Pi_1^{\text{in}} = 0, \Pi_2^{\text{in}} \neq 0$ , can be treated in a similar way as in the previous section. Using the first edge condition in Eq. (13) and noting that  $\overline{\Pi}_1^{\text{out}} = 0$  [see Eq. (22)], we obtain

$$\partial_\xi \overline{\Pi}_1^{\text{out}} = 0 \quad \text{for} \quad \xi = \eta = 0. \quad (52)$$

Expanding  $\overline{\Pi}_1^{\text{out}}$  in terms of spheroidal waves as in Eq. (23) and expressing  $A_{n, m_0}$  as in Eq. (26), we get

$$\alpha^{n_0, m_0}sa_1^{m_0}(\gamma) + \beta^{n_0, m_0}sb_1^{m_0}(\gamma) = 0, \quad (53)$$

where the functions  $sa_1$  and  $sb_1$  are given by Eqs. (45) and (46).

As we explained in the previous section, for  $m_0 = 0$  we have to set  $\alpha^{n_0, 0} = 0$ , since otherwise  $\partial_\xi \Pi_1$  will fail to converge at  $\xi = 0, \eta = \pm 1$ , leading to a diverging electromagnetic field in the middle of the disk. Consequently  $\beta^{n_0, 0}$  has to vanish in order to satisfy Eq. (53), meaning that  $\Pi_1^{\text{out}} = 0$ .

Let us now restrict to  $m_0 \neq 0$  and express  $\beta^{n_0, m_0}$  as

$$\beta^{n_0, m_0} = -q_2^{m_0}(\gamma)\alpha^{n_0, m_0}. \quad (54)$$

The function  $q_2^{m_0}$  can be easily calculated from Eq. (53) and is independent of  $n_0$ ,

$$q_2^{m_0}(\gamma) = \frac{sa_1^{m_0}(\gamma)}{sb_1^{m_0}(\gamma)}. \quad (55)$$

The expansion of the functions  $sa_1$  and  $sb_1$  for small  $\gamma$  is given in the previous section. The remaining edge condition

$$\partial_\eta (\overline{\Pi}_2^{\text{sc}} + \overline{\overline{\Pi}}_2^{\text{sc}}) = 0 \quad \text{for} \quad \xi = \eta = 0 \quad (56)$$

fixes  $\alpha^{n_0, m_0}$ . Similarly to Eq. (44) we get

$$\alpha_2^{n_0, m_0}(\gamma) = \frac{S_{n_0}^{\prime m_0(3)}(-i0)Sp_{n_0}^{\prime m_0}(0)S_{n_0}^{\prime m_0(1)}(-i0)}{[sa_2^{n, m_0} - q_2^{m_0}sb_2^{n, m_0}]S_{n_0}^{\prime m_0(3)}(-i0)}. \quad (57)$$

Note again the subscript that we added to  $\alpha^{n_0, m_0}$  in order not to confuse the different functional forms in Eq. (44) and (57).

The case  $m_0 = 0$  again needs special treatment. Since  $a_2^{n, m_0}$  vanishes identically for  $m_0 = 0$  [see Eq. (30)], Eq. (27) reduces to  $B_n^{n_0, 0} = \beta^{n_0, 0} b_2^{n, 0}$ , where we have dropped the tilde on  $\beta^{n_0, 0}$ . We then have

$$\beta_2^{n_0, 0}(\gamma) = \frac{S_{n_0}^{(3)}(-i0) S_{n_0}^{'(0)}(0) S_{n_0}^{'(1)}(-i0)}{s b_2^{n_0, 0} S_{n_0}^{'(3)}(-i0)}. \quad (58)$$

As described above, we set  $\partial_\xi \bar{\Pi}_2^{sc} \sim \delta(1 - \eta^2)$  for  $\xi = 0$ . Then

$$\bar{\Pi}_2^{sc} = \beta^{n_0, 0} \sum_{n=0}^{\infty} b_2^{n, 0}(\gamma) S_n^{(0)(3)}(-i\xi) S_p_n^0(\eta), \quad (59)$$

where  $\beta^{n_0, 0}$  is fixed by

$$\begin{aligned} & -S_{n_0}^{(3)}(-i0) S_{n_0}^{'(0)}(0) \frac{S_{n_0}^{'(1)}(-i0)}{S_{n_0}^{'(3)}(-i0)} \\ & + \beta^{n_0, 0} \sum_{n=1}^{\infty} b_2^{n, 0}(\gamma) S_n^{(0)(3)}(-i0) S_p_n^{'(0)}(0) = 0. \end{aligned} \quad (60)$$

## B. The T-matrix elements

Having found the complete solution of the scattering problem, we can express our results in terms of the T-matrix. The T-matrix depends on the product  $\gamma = kR$  and the quantum numbers  $n$  and  $m$ . For large distances from the disk,  $k \ll 1/R$ , the spheroidal modes become spherical modes, which can be of two types: electrical (E) modes (also called TM modes) and magnetic (M) modes (also called TE modes). This decomposition is a general property of Debye potentials. The potential  $\Pi_1$  alone yields a magnetic field with vanishing radial component (TM or E modes), while the potential  $\Pi_2$  corresponds to a vanishing radial component of the electric field (TE or M modes). Therefore, the T-matrix can be split into four submatrices,  $T^{EE}$ ,  $T^{MM}$ ,  $T^{EM}$ , and  $T^{ME}$ . In the following we show how the T-matrix can be constructed from the results in the previous sections.

### 1. The case $\Pi_1^{\text{in}} \neq 0, \Pi_2^{\text{in}} = 0$

As we have seen, the incoming mode  $\Pi_1^{(\text{in})}$  generates outgoing fields  $\Pi_1^{(\text{out})}$  and  $\Pi_2^{(\text{out})}$ . The total potentials  $\Pi_1$  and  $\Pi_2$  are a superposition of the incoming and outgoing fields and may be written as

$$\Pi_1 = \Pi_{n_0}^{m_0(\text{in})} + \sum_{n, m} T_{n, m, n_0, m_0}^{EE} \Pi_n^{m(\text{out})}, \quad (61)$$

$$\Pi_2 = 0 + \sum_{n, m} T_{n, m, n_0, m_0}^{ME} \Pi_n^{m(\text{out})}. \quad (62)$$

Let us first consider the case  $m_0 \neq 0$ . From Eqs. (21), (23), and (24) we find

$$\begin{aligned} T_{n, m, n_0, m_0}^{EE} = & -\frac{S_{n_0}^{m_0(1)}(-i0)}{S_{n_0}^{m_0(3)}(-i0)} \delta_{n, n_0} \delta_{m, m_0} \\ & + \alpha_1^{n_0, m_0} (a_1^{n, m_0} - q_1^{m_0} b_1^{n, m_0}) \delta_{m, m_0} \end{aligned} \quad (63)$$

and

$$T_{n, m, n_0, m_0}^{ME} = \alpha_1^{n_0, m_0} (a_2^{n, m_0} - q_1^{m_0} b_2^{n, m_0}) \delta_{m, m_0}. \quad (64)$$

Note that all functions depend on  $\gamma$ .

For  $m_0 = 0$ , the matrix  $T^{ME}$  vanishes, whereas  $T^{EE}$  becomes

$$T_{n, m, n_0, 0}^{EE} = -\frac{S_{n_0}^{(1)}(-i0)}{S_{n_0}^{(3)}(-i0)} \delta_{n, n_0} \delta_{m, 0} + \beta_1^{n_0, 0} b_1^{n, 0} \delta_{m, 0}. \quad (65)$$

For the Casimir interaction at large distances, it is useful to know the behavior of the T-matrix at small  $\gamma$ . For the elements of the  $T^{EE}$  and  $T^{ME}$  matrices we find for  $m_0 > 0$  the scaling

$$\frac{S_{n_0}^{m_0(1)}(-i0)}{S_{n_0}^{m_0(3)}(-i0)} \sim O(\gamma^{2n_0+1}), \quad (66)$$

$$\begin{aligned} & \alpha_1^{m_0, n_0} (a_1^{n, m_0} - q_1^{m_0} b_1^{n, m_0}) \\ & \sim O(\gamma^{n_0}) [O(\gamma^{n+1}) - O(\gamma^{n+3})], \end{aligned} \quad (67)$$

$$\begin{aligned} & \alpha_1^{m_0, n_0} (a_2^{n, m_0} - q_1^{m_0} b_2^{n, m_0}) \\ & \sim O(\gamma^{n_0}) [O(\gamma^{n+2}) - O(\gamma^{n+4})]. \end{aligned} \quad (68)$$

For nonvanishing  $T^{EE}$  elements,  $n_0 - m_0$  and  $n - m_0$  have to be even. For nonvanishing  $T^{ME}$  elements,  $m_0$  has to be larger than 0 and  $n_0 - m_0$  even and  $n - m_0$  odd. The matrix elements of order  $O(\gamma^3)$  are  $T_{0, 0, 2, 0}^{EE} = 4\gamma^3/45i\pi$  and  $T_{1, 1, 1, 1}^{EE} = T_{1, -1, 1, -1}^{EE} = 8i\gamma^3/9\pi$ .

We now define the vector modes

$$\mathbf{M}_n^m = \nabla \times (\mathbf{r} \Pi_n^m), \quad \mathbf{N}_n^m = \frac{1}{ik} \nabla \times \nabla \times (\mathbf{r} \Pi_n^m), \quad (69)$$

so that we can write the  $\mathbf{E}$  field in the usual form that defines the T-matrix,

$$\frac{\mathbf{E}}{ik} = \mathbf{N}_{n_0}^{m_0(\text{in})} + \sum_{n, m} (T_{n, m, n_0, m_0}^{EE} \mathbf{N}_n^{m(\text{out})} + T_{n, m, n_0, m_0}^{ME} \mathbf{M}_n^{m(\text{out})}), \quad (70)$$

showing that our definition agrees with the one used usually for vector spherical waves.

### 2. The case $\Pi_2^{\text{in}} \neq 0, \Pi_1^{\text{in}} = 0$

The matrices  $T^{MM}$  and  $T^{EM}$  can be found as in the case before. The T-matrix elements are now defined by

$$\Pi_2 = \Pi_{n_0}^{m_0(\text{in})} + \sum_{n, m} T_{n, m, n_0, m_0}^{MM} \Pi_n^{m(\text{out})}, \quad (71)$$

$$\Pi_1 = 0 + \sum_{n, m} T_{n, m, n_0, m_0}^{EM} \Pi_n^{m(\text{out})}. \quad (72)$$

We again first consider the case  $m_0 \neq 0$  and obtain

$$\begin{aligned} T_{n, m, n_0, m_0}^{MM} = & -\frac{S_{n_0}^{m_0(1)}(-i0)}{S_{n_0}^{m_0(3)}(-i0)} \delta_{n, n_0} \delta_{m, m_0} \\ & + \delta_{m, m_0} \alpha_2^{n_0, m_0} (a_2^{n, m_0} - q_2^{m_0} b_2^{n, m_0}) \end{aligned} \quad (73)$$

and

$$T_{n, m, n_0, m_0}^{EM} = \alpha_2^{n_0, m_0} (a_1^{n, m_0} - q_2^{m_0} b_1^{n, m_0}) \delta_{m, m_0}. \quad (74)$$

For  $m_0 = 0$ , the matrix  $T^{\text{EM}}$  vanishes, whereas  $T^{\text{MM}}$  simplifies to

$$T_{n,m,n_0,0}^{\text{MM}} = -\frac{S_{n_0}^{\prime(1)}(-i0)}{S_{n_0}^{\prime(3)}(-i0)}\delta_{n,n_0}\delta_{m,0} + \beta_2^{n_0,0}b_2^{n,0}\delta_{m,0}. \quad (75)$$

For the elements of the  $T^{\text{MM}}$  and  $T^{\text{EM}}$  matrices we find, for  $m > 0$  at small  $\gamma$ , the scaling

$$\frac{S_{n_0}^{\prime(1)}(-i0)}{S_{n_0}^{\prime(3)}(-i0)} \sim O(\gamma^{2n_0+1}), \quad (76)$$

$$\alpha_2^{m_0,n_0}(a_2^{n,m_0} - q_2^{m_0}b_2^{n,m_0}) \sim O(\gamma^{n_0+1})[O(\gamma^{n+2}) - O(\gamma^n)], \quad (77)$$

$$\alpha_2^{m_0,n_0}(a_1^{n,m_0} - q_2^{m_0}b_1^{n,m_0}) \sim O(\gamma^{n_0+1})[O(\gamma^{n+1}) - O(\gamma^{n+1})]. \quad (78)$$

For the nonvanishing  $T^{\text{MM}}$  elements  $n_0 - m_0$  and  $n - m_0$  have to be odd, and for the nonvanishing  $T^{\text{EM}}$  elements  $m_0$  has to be larger than 0 and  $n_0 - m_0$  odd and  $n - m_0$  even. The only matrix element of  $O(\gamma^3)$  is  $T_{1,0,1,0}^{\text{MM}} = 4\gamma^3/9i\pi$ . (Without the contribution from the edge, we would have obtained  $T_{1,0,1,0}^{\text{MM}} = -2\gamma^3/9i\pi$ .)

Finally, with the definitions of Eq. (69), the  $\mathbf{E}$  field can be written as

$$\frac{\mathbf{E}}{ik} = \mathbf{M}_{n_0}^{m_0(\text{in})} + \sum_{n,m} (T_{n,m,n_0,m_0}^{\text{EM}} \mathbf{N}_n^{m(\text{out})} + T_{n,m,n_0,m_0}^{\text{MM}} \mathbf{M}_n^{m(\text{out})}), \quad (79)$$

which corresponds to the usual definition of T-matrix elements.

### C. Symmetry and unitarity of the T-matrix

Because they are not eigenstates of  $\hat{L}^2$ , the modes in Eq. (69) with the same  $m$  are not orthogonal, and so the T-matrix does not have the usual symmetry and unitarity properties in this basis. The asymmetry is particularly pronounced for the case where  $n \neq 0$  and  $n_0 = m = 0$ : these matrix elements begin at higher order in  $\gamma$  than the corresponding ones with  $n = m = 0$  and  $n_0 \neq 0$ . This discrepancy can be traced to the behavior of the  $b_1$  coefficient in Eq. (29). Although it appears to be  $O(\gamma)$ , as we discuss below, an expansion in  $\gamma$  yields an expansion of the angular spheroidal in terms of Legendre functions; their orthogonality properties in turn lead to a cancellation of the leading orders in  $\gamma$ . The true behavior is given by the exact expression for the integral in the case where  $m = 0$ , given in Eq. (A1), which is  $O(\gamma^{2n+1})$ .

As a result, it is helpful to convert the T-matrix to the basis of spherical vector waves. There exist several normalization conventions; we use those of Emig *et al.* [21]. The vector spherical wave functions then read, for an imaginary wave number  $k = i\kappa$  (which is useful for the Casimir energy computation below),

$$\mathbf{M}_{lm}^{(\text{reg})}(\kappa, \mathbf{r}) = \frac{1}{\sqrt{l(l+1)}} \nabla \times (\phi_{lm}^{(\text{reg})}(\kappa, \mathbf{r}) \mathbf{r}), \quad (80)$$

$$\mathbf{M}_{lm}^{(\text{out})}(\kappa, \mathbf{r}) = \frac{1}{\sqrt{l(l+1)}} \nabla \times (\phi_{lm}^{(\text{out})}(\kappa, \mathbf{r}) \mathbf{r}), \quad (81)$$

$$\mathbf{N}_{lm}^{(\text{reg})}(\kappa, \mathbf{r}) = \frac{1}{\kappa \sqrt{l(l+1)}} \nabla \times \nabla \times (\phi_{lm}^{(\text{reg})}(\kappa, \mathbf{r}) \mathbf{r}), \quad (82)$$

$$\mathbf{N}_{lm}^{(\text{out})}(\kappa, \mathbf{r}) = \frac{1}{\kappa \sqrt{l(l+1)}} \nabla \times \nabla \times (\phi_{lm}^{(\text{out})}(\kappa, \mathbf{r}) \mathbf{r}), \quad (83)$$

where the modified spherical wave functions are

$$\phi_{lm}^{(\text{reg})}(\kappa, \mathbf{r}) = i_l(\kappa|\mathbf{r}|)Y_{lm}(\hat{\mathbf{r}}), \quad (84)$$

$$\phi_{lm}^{(\text{out})}(\kappa, \mathbf{r}) = k_l(\kappa|\mathbf{r}|)Y_{lm}(\hat{\mathbf{r}}). \quad (85)$$

Here,  $i_l(z) = \sqrt{\frac{\pi}{2z}} I_{l+1/2}(z)$  is the modified spherical Bessel function of the first kind, and  $k_l(z) = \sqrt{\frac{2}{\pi z}} K_{l+1/2}(z)$  is the modified spherical Bessel function of the third kind.

It is important to note three differences between the definition of the spherical basis and that of the spheroidal basis, one of which is nontrivial:

(1) The spherical basis has been written in terms of modified radial functions, the conventions for which introduce powers of  $i$  relative to the ordinary functions with imaginary wave number.

(2) The spherical waves have been written in terms of spherical harmonics, which include a factor of  $\sqrt{\frac{N_{l,m}}{2\pi}}$  compared to the corresponding expression in terms of Legendre functions, the analog of which is used in the spheroidal waves. [For the definition of the factor  $N_{l,m}$ , see Eq. (32)].

(3) The nontrivial difference is the normalization factor of  $\frac{1}{\sqrt{l(l+1)}}$ . Because the spheroidal functions are not eigenstates of  $\hat{L}^2$ , no direct analog of this quantity exists in the spheroidal case. (The spheroidal eigenvalue plays a similar role in separation of variables for the scalar wave equation, but that quantity does not yield a corresponding normalization of the vector spheroidal functions.) It is the introduction of this quantity in converting to spherical waves that renders the resulting basis orthonormal. We note also that while the spheroidal basis starts with  $n = 0$ , the spherical basis starts at  $l = 1$ .

To convert to the spherical basis, we begin from the expansion of the spheroidal angular functions in terms of Legendre functions,

$$Sp_n^m(\eta; i\gamma) = \sum_{v \geq |m|}^{\infty} i^{v-n} A_{n,v}^m(i\gamma) P_v^m(\eta), \quad (86)$$

where the expansion coefficients  $A_{n,v}^m$  are obtained via recursion relations [37]. If  $m$  is even (odd), the summation runs over even (odd)  $v$  only, and the coefficient  $A_{n,v}^m$  is  $O(\gamma^v)$  for small  $\gamma$ . Note that the transformation matrix does not depend on any coordinate. This fact can be used to obtain the transformation formulas for spheroidal waves. At large  $\xi$ , the radial spheroidal functions simplify to

$$S_n^{(1)}(-i\xi; i\gamma) \sim \frac{1}{\gamma\xi} \cos\left(\gamma\xi - \frac{n+1}{2}\pi\right), \quad (87)$$

$$S_n^{(3)}(-i\xi; i\gamma) \sim \frac{1}{\gamma\xi} \exp\left[+i\left(\gamma\xi - \frac{n+1}{2}\pi\right)\right]. \quad (88)$$



Multiplying Eq. (86) by  $S_n^{m(j)}(-i\xi; i\gamma) e^{im\varphi}$  yields the following transformation between scalar waves,

$$L_n^{m(j)}(\xi, \eta, \varphi; i\gamma) = \sum_{v \geq |m|}^{\infty} A_{n,v}^m(i\gamma) \psi_v^{(j)}(kr) P_v^m(\cos \theta) e^{im\varphi}, \quad (89)$$

where  $\psi_v$  denotes the spherical Hankel function of type  $j$ . To verify Eq. (89), we use the asymptotic expansions of  $S_n^{m(j)}(-i\xi; i\gamma)$  at large  $\xi$ . One then immediately realizes that Eq. (89) holds for large  $\xi$ . Since the transformation matrix  $A_{n,v}^m$  does not depend on any coordinate, the relation obtained must also hold at any  $\xi$ .

The transformation inverse to Eq. (89) can be found again in the limit of large  $\xi$ , in which case the radial functions can be canceled on both sides. Expanding the  $Sp$  functions as in Eq. (86) and using the orthogonal relations for the Legendre polynomials similar to those in Eq. (25) for spheroidal angular functions yields

$$[A^{-1}]_{v,n}^m(i\gamma) = \frac{N_{n,m}}{N_{v,m}} A_{n,v}^m(i\gamma). \quad (90)$$

The inverse matrix is, as expected, the transposed matrix multiplied by normalization factors.

Since the transformation matrix does not depend on any coordinate, the same transformation matrix also transforms between vector waves. We just let the operator  $\nabla \times (\mathbf{r} \dots)$  and  $\nabla \times \nabla \times (\mathbf{r} \dots)$  act on Eq. (89), passing through the matrix  $A_{n,v}^m$ .

#### D. The T-matrix in the spherical basis

To transform to the spherical basis, we first form a rescaled T-matrix, denoted  $\mathcal{T}$ , in which each matrix element found above is multiplied by a factor of  $i^{n_0-n} \sqrt{\frac{N_{n_0,m}}{N_{n,m}}}$  to address the first two differences between the bases listed above. This scaling makes manifest the symmetry in  $m \rightarrow -m$ . We then use the following matrix that describes the change of basis,

$$M_{lm_l n m_n}^{P_l P_n} = \delta_{m_l m_n} \delta_{P_l P_n} \sqrt{l(l+1)} \times \sqrt{\frac{N_{n,m_n}}{N_{l,m_l}}} (-1)^{(l-n)/2} A_{l,n}^m(i\gamma), \quad (91)$$

to convert between the spheroidal basis, indexed by  $n, m_n$ , and polarization  $P_n$ , and the spherical basis, indexed by  $l, m_l$ , and polarization  $P_l$ . Note that the spherical index  $l$  starts from 1, while the spheroidal index  $n$  starts from 0. The corresponding inverse transformation is given by

$$[M^{-1}]_{nm_n lm_l}^{P_n P_l} = \delta_{nm_n lm_l} \delta_{P_n P_l} \frac{1}{\sqrt{l(l+1)}} \times \sqrt{\frac{N_{n,m_n}}{N_{l,m_l}}} (-1)^{(l-n)/2} A_{l,n}^m(i\gamma). \quad (92)$$

We note that the prefactor  $[l(l+1)]^{\pm 1/2}$ , which addresses the third difference between the spheroidal basis and the spherical basis listed above, is implemented via the spherical index  $l$ , which is never 0. We thus obtain the T-matrix in the spherical

basis as  $\tilde{T} = M T M^{-1}$ , which has the usual symmetry and unitarity properties.

### III. THE TRANSLATION MATRIX AND THE CASIMIR ENERGY

Having converted the T-matrix elements to the spherical basis, we are now prepared to evaluate the Casimir energy of a disk that is parallel to an infinite plane, using techniques developed for the sphere-plane problem [21,39,40]. In this approach, the Casimir energy is given as

$$E = \frac{\hbar c}{2\pi} \int_0^\infty d\kappa \ln \det(1 - \tilde{T}\tilde{U}), \quad (93)$$

where  $\tilde{T}$  is the T-matrix of the disk in spherical coordinates and  $\tilde{U}$  combines the reflection coefficient  $r$  for the plane (see below) and the conversion matrix  $D$ , which expresses spherical vector waves centered at the origin of the disk in terms of planar vector waves centered at the plane. The matrix elements of  $\tilde{U}$  are given by

$$\begin{aligned} \tilde{U}_{lm' m'}^{P P'} &= \int_0^\infty \frac{k_\perp dk_\perp}{2\pi} \frac{e^{-2d\kappa_\parallel}}{2\kappa\kappa_\parallel} \delta_{mm'} \\ &\times \sum_Q D_{lm P, k_\perp Q} r^Q(\kappa, \kappa_\parallel) \chi_{P'} \chi_Q D_{l' - m' P', k_\perp Q}, \end{aligned} \quad (94)$$

where  $d$  is the distance from the center of the disk to the plane,  $Q$  is the polarization of the plane wave,  $\chi_P$  is  $+1$  for electric modes and  $-1$  for magnetic modes,  $\kappa_\parallel = \sqrt{k_\perp^2 + \kappa^2}$ ,  $r^Q(\kappa, \kappa_\parallel)$  is the Fresnel reflection coefficient for scattering from the plane, and

$$D_{lm P, k_\perp Q} = \sqrt{\frac{4\pi N_{l,m}}{l(l+1)}} \begin{cases} \frac{k_\perp}{\kappa} P_l^{m'}\left(\frac{\kappa_\parallel}{\kappa}\right) & \text{for } P = Q, \\ \frac{im\kappa}{k_\perp} \chi_P P_l^m\left(\frac{\kappa_\parallel}{\kappa}\right) & \text{for } P \neq Q \end{cases} \quad (95)$$

gives the conversion between vector spherical waves and vector plane waves in terms of the associated Legendre functions  $P_l^m$  and its derivative  $P_l^{m'}$  with respect to its argument. For a perfectly conducting plane,  $r^Q(\kappa, \kappa_\parallel) = \chi_Q = \pm 1$  for electric and magnetic modes, respectively.

This expression is now suitable for numerical evaluation, which we carry out in Mathematica, using routines for computing spheroidal functions [35,41] based on the package created by Falloon [42]. This code provides all the necessary spheroidal functions, as well as the expansion coefficients  $A_{v,n}^m(i\gamma)$ . Since we are carrying out this calculation via a conversion to the spherical basis, we are restricted to configurations with  $d > R$ , so that a sphere enclosing the disk does not intersect the plane [21]. Our calculation shows the corresponding numerical instabilities for  $d < R$ .

#### A. Rotated disk

The translation matrix elements in Eq. (94) are obtained from the expansion of a plane wave constructed with “pilot vector”  $\hat{\mathbf{z}}$  in terms of transverse spherical vector modes, which

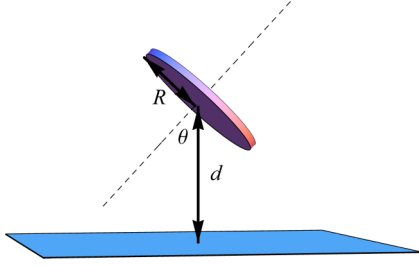


FIG. 1. Geometry of the disk for separation  $d$ , radius  $R$ , and orientation angle  $\theta$ .

are plane waves with wave vector

$$\begin{aligned} \mathbf{k} &= i\kappa(\sin\theta_k \cos\phi_k, \sin\theta_k \sin\phi_k, \cos\theta_k) \\ &= (k_\perp \cos\phi_k, k_\perp \sin\phi_k, i\kappa_\parallel). \end{aligned} \quad (96)$$

By rotating the  $z$  axis of the spherical modes to an angle  $\theta$  from the normal to the plane, we can obtain the Casimir energy for a disk whose normal is tilted by that angle  $\theta$  away from the normal to the plane, allowing us to extend the results found previously for scalar fields [35]. We choose to rotate around the  $y$  axis, as shown in Fig. 1. In these coordinates, the pilot vector becomes  $(\sin\theta, 0, \cos\theta)$ , and

$$\mathbf{k} = i\kappa(\sin\theta_q \cos\phi_q, \sin\theta_q \sin\phi_q, \cos\theta_q), \quad (97)$$

where

$$\theta_q = \arccos \frac{i\kappa_\parallel \cos\theta - k_\perp \cos\phi_k \sin\theta}{i\kappa}, \quad (98)$$

$$\phi_q = \arctan \frac{k_\perp \sin\phi_k}{k_\perp \cos\phi_k \cos\theta + i\kappa_\parallel \sin\theta}. \quad (99)$$

The only change to the calculation is that we now have

$$\tilde{\mathcal{U}}_{lm'l'm'}^{PP'}(\theta) = \int_0^\infty \frac{d^2\mathbf{k}_\perp}{(2\pi)^2} \frac{e^{-2d\kappa_\parallel}}{2\kappa\kappa_\parallel} \sum_Q D_{lmP, \mathbf{k}_\perp Q}(\theta) r^Q(\kappa, \kappa_\parallel) \chi_{P'} \chi_Q D_{l'-m'P', \mathbf{k}_\perp Q}(-\theta), \quad (100)$$

where

$$D_{lmP, \mathbf{k}_\perp Q}(\theta) = e^{im\phi_q} \sqrt{\frac{4\pi N_{l,m}}{l(l+1)}} \frac{\kappa}{k_\perp} \left[ im P_l^m(\cos\theta_q) \frac{\sin\theta \sin\phi_q}{\sin\theta_q} + P_l^{m'}(\cos\theta_q) \sin\theta_q (\cos\theta_q \cos\phi_q \sin\theta - \cos\theta \sin\theta_q) \right] \quad (101)$$

for  $P = Q$ , and

$$D_{lmP, \mathbf{k}_\perp Q}(\theta) = e^{im\phi_q} \sqrt{\frac{4\pi N_{l,m}}{l(l+1)}} \frac{\kappa}{k_\perp} \left[ im P_l^m(\cos\theta_q) \left( \cos\theta - \frac{\cos\phi_q \cos\theta_q \sin\theta}{\sin\theta_q} \right) + P_l^{m'}(\cos\theta_q) \sin\theta \sin\theta_q \sin\phi_q \right] \quad (102)$$

for  $P \neq Q$ . As in the case of  $\theta = 0$ , these expressions are obtained as the dot product of the spherical wave and the corresponding vector spherical harmonic of  $\hat{\mathbf{k}}$  in the expansion of a plane wave [43,44]. For any angle  $\theta$ , the calculation still requires  $d < R$ , so that a sphere enclosing the disk does not intersect the plane. As a result, for  $\theta = \pi/2$ , we could consider a disk whose edge is arbitrarily close to the plane. However, as the edge approaches the plane, more partial waves and larger values of  $\kappa$  are required to accurately compute the infinite sums and integrals.

We note that for  $\theta \neq 0$ , careful attention is needed to avoid problems arising from branch cuts. In particular, Eqs. (101) and (102) can be expressed in terms of  $k_\perp, \kappa_\parallel, \kappa, \phi_k$ , and  $\theta$  without the need for any inverse trigonometric functions. Similarly, one must take care to obtain the appropriate analytic continuation of the Legendre functions outside the unit circle.

### B. Large separations

For  $d \gg R$ , the Casimir energy is dominated by the contribution from long wavelengths, corresponding to small  $\gamma$ . The lowest-order contributions to the T-matrix are  $O(\gamma^3)$ ,  $T_{0,0,2,0}^{EE} = 4\gamma^3/45i\pi$ ,  $T_{1,1,1,1}^{EE} = T_{1,-1,1,-1}^{EE} = 8i\gamma^3/9\pi$ , and  $T_{1,0,1,0}^{MM} = 4\gamma^3/9i\pi$ . However,  $T_{0,0,2,0}^{EE}$  does not contribute at lowest order: Since there is no  $l = 0$  mode in the spherical basis, its effect enters through off-diagonal terms mixing different values of  $l$  and  $n$ , which introduce additional

powers of  $\gamma$ . The values of  $T_{1,1,1,1}^{EE} = T_{1,-1,1,-1}^{EE}$  and  $T_{1,0,1,0}^{MM}$  correspond to the static electric and magnetic dipole responses respectively,  $\alpha_E = 4R^3/3\pi$  and  $\alpha_M = -2R^3/3\pi$ , which agree with previous results [45]. Using the same approach as in the sphere-plane geometry [39], we obtain the Casimir energy in the long-distance limit for  $\theta = 0$  as

$$\mathcal{E} = -\frac{\hbar c}{8\pi d^4} (2\alpha_E - \alpha_M) + O\left(\frac{1}{d^6}\right). \quad (103)$$

Higher-order terms are more difficult to obtain, because they require resummation of the infinite sums in  $sa_1^m, sb_1^m, sa_2^m$ , and  $sb_2^m$  at the appropriate order in  $\gamma$ .

## IV. RESULTS

Figure 2 shows the Casimir energy for a perfectly conducting disk of radius  $R$  and a perfectly conducting plane, as a function of the rotation angle for different separations  $d/R$ . To facilitate the comparison between different separation distances, the energies have been scaled by a factor of  $d^3$ , since a  $d^{-3}$  decay is predicted by the proximity force approximation (PFA). The plots range from  $\theta = 0$ , when the disk is parallel to the plane, to  $\theta = \pi/2$ , when the disk is perpendicular to the plane, and from  $d = 1.5 R$  to  $d = 4.0 R$ . We note that at these separations, the full energy for  $\theta = 0$  is still significantly

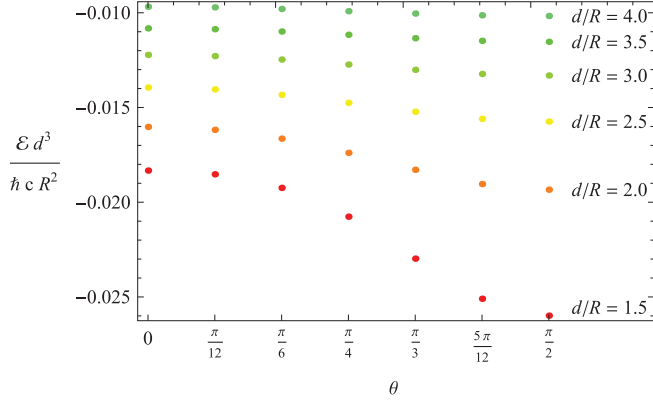


FIG. 2. Scaled Casimir energy for a perfectly conducting disk of radius  $R$  opposite a perfectly conducting plane, where the center of the disk is at a distance  $d$  from the plane and the normal to the disk is at an angle  $\theta$  relative to the normal to the plane. The energies have been scaled by  $d^3$  to facilitate comparison.

smaller in magnitude than the prediction of the PFA,

$$\mathcal{E}_{\text{PFA}} = -\frac{\hbar c}{d^3} \frac{\pi^2}{720} \pi R^2, \quad (104)$$

which on this graph would correspond to a value of  $-\frac{\pi^3}{720} \approx -0.043$ , independent of  $d$ . In these calculations, we have truncated the numerical sums after  $n_{\text{max}} = l_{\text{max}} = 5$  and used the interval  $[\frac{1}{128R}, \frac{4}{R}]$  for the integral over  $\kappa$ , and we have checked that the results are not sensitive to these choices. (The dimensionless ratio  $\mathcal{E}/\mathcal{E}_{\text{PFA}}$  must be a function of the dimensionless quantities  $d/R$  and  $\theta$ .)

For the case where the disk is parallel to the plane, Fig. 3 shows a comparison of our result for the Casimir energy and the PFA prediction. We also show numerical results obtained

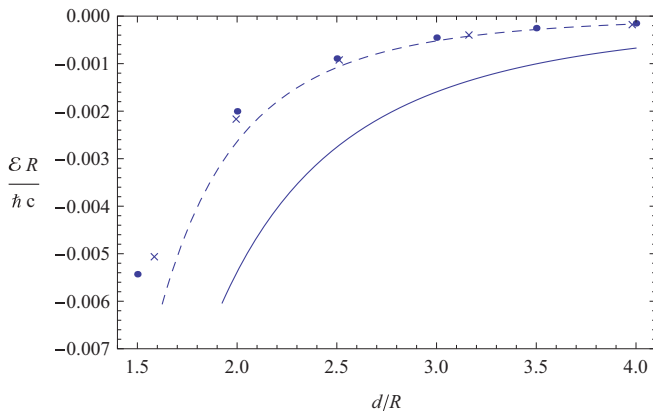


FIG. 3. Casimir energy for a perfectly conducting disk of radius  $R$  parallel to a perfectly conducting plane, where the center of the disk is at a distance  $d$  from the plane. Black circles represent our results; crosses represent the fluctuating-surface-current calculation from Ref. [32]; the dotted line represents the dipole approximation, given in Eq. (103); and the solid line represents the PFA, given in Eq. (104).

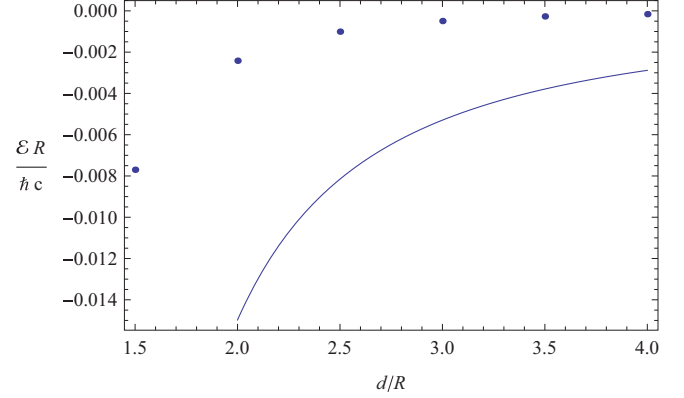


FIG. 4. Casimir energy for a perfectly conducting disk of radius  $R$  perpendicular to a perfectly conducting plane, where the center of the disk is at a distance  $d$  from the plane. Black circles represent our results and the solid line represents the “edge PFA” from Ref. [25].

by using the fluctuating-surface-current method [32].<sup>2</sup> The two exact methods agree well, demonstrating that the magnitude of the energy is significantly smaller than the PFA prediction. For the case when the disk is perpendicular to the plane, the Casimir energy is shown in Fig. 4. We see that the result is also smaller than the “edge PFA”, based on the result for a half-plane with a sharp edge opposite an infinite plane [25],

$$\mathcal{E}_{\text{ePFA}} = -0.0067415 \hbar c \pi \sqrt{\frac{R}{2(d-R)^3}}. \quad (105)$$

## V. CONCLUSIONS

Building on Meixner’s analysis of diffraction from a disk [36], we have constructed the full scattering T-matrix for the scattering of light from a perfectly conducting disk, which we have then expressed in a vector spherical wave basis, a calculation that requires particular attention to finite contributions arising from singular terms in the  $m = 0$  channel. This result represents one of the few cases of a nondiagonal T-matrix that can be computed exactly in closed form. The scattering approach then allows us to use this information to obtain Casimir interaction energies for systems such as the disk-plane geometry we have considered here, for arbitrary orientations of the disk. This approach is particularly valuable for configurations where edge effects are important, such as the case where the disk is perpendicular to the plane, since there one cannot use a gradient expansion for gently curved surfaces [46,47]. We have found that the PFA result significantly overestimates the Casimir energy at intermediate distances, as does the “edge PFA” based on the result for a half-plane.

While conversion to the vector spherical basis facilitates the consideration of different rotation angles, it limits the calculation to  $d > R$ , to ensure that a sphere enclosing the

<sup>2</sup>This calculation is implemented in the SCUFF-EM package, available at <http://GitHub.com/HomerReid/SCUFF-EM>.

disk does not intersect the plane. In order to allow  $d < R$ , one must consider instead the vector spheroidal basis, which is not orthonormal. Since the scattering method relies on a mode expansion of the free Green's function, it cannot be applied directly to the spheroidal basis; as a result, an important direction for future work is to generalize the scattering method to include this case.

### ACKNOWLEDGMENTS

This work is based on preliminary studies of the scattering problem for a disk by Alexej Weber in an earlier stage of this project. His contribution is acknowledged. We thank G. Bimonte, R. L. Jaffe, M. Kardar, and M. Krüger for helpful discussions and M. T. H. Reid for carrying out comparisons with the methods of Ref. [32]. N.G. was supported in part by the National Science Foundation (NSF) through Grant No. PHY-1520293.

### APPENDIX: USEFUL INTEGRALS

Here we collect useful integrals, obtained from [48–50]. For  $m = 0$ , we have the closed-form integrals

$$\int_{-1}^1 S_p^0(\eta; i\gamma) \frac{\sin(\gamma \sqrt{1-\eta^2})}{\sqrt{1-\eta^2}} d\eta = 2\gamma S_n^{0(1)}(0; i\gamma)^2 A_n^m(i\gamma) \quad (\text{A1})$$

and

$$\int_{-1}^1 S_p^0(\eta; i\gamma) \frac{\cos(\gamma \sqrt{1-\eta^2})}{\sqrt{1-\eta^2}} d\eta = 2\gamma S_n^{0(1)}(0; i\gamma) S_n^{0(2)}(0; i\gamma) A_n^m(i\gamma), \quad (\text{A2})$$

where the normalization factor  $A_n^m(i\gamma)$  is given by

$$A_n^m(i\gamma) = \sum_{v \geq |m|} i^{v-n} A_{n,v}^m(i\gamma). \quad (\text{A3})$$

We can also simplify the leading-order subtractions using the integrals

$$\int_{-1}^1 P_l^m(x) dx = \frac{(-1)^l 2^{m-1} m \Gamma(\frac{l}{2}) \Gamma(\frac{l+m+1}{2})}{\Gamma(\frac{l+3}{2}) (\frac{l-m}{2})!} \quad (\text{A4})$$

and

$$\int_{-1}^1 \frac{P_l^m(x)}{\sqrt{1-x^2}} dx = \frac{2^m \pi (-1)^{\frac{m-l}{2}} \Gamma(\frac{l+1}{2})}{\Gamma(\frac{1-m-l}{2}) \Gamma(1+\frac{l}{2}) (\frac{l-m}{2})!}, \quad (\text{A5})$$

where from these results we can also obtain

$$\int_{-1}^1 \frac{x P_l^m(x)}{\sqrt{1-x^2}} dx = \frac{2^m \pi (-1)^{\frac{m-l-1}{2}} \Gamma(\frac{l}{2})}{\Gamma(-\frac{m}{2}-\frac{l}{2}) \Gamma(\frac{l+3}{2}) \Gamma(\frac{1-m+l}{2})} \quad (\text{A6})$$

and

$$\int_{-1}^1 \frac{x P_l^m(x)}{1-x^2} dx = \frac{2^{m+1} \pi (-1)^{\frac{m-l-1}{2}} \Gamma(\frac{l+1}{2})}{m \Gamma(-\frac{m}{2}-\frac{l}{2}) \Gamma(1+\frac{l}{2}) \Gamma(\frac{1-m+l}{2})} \quad (\text{A7})$$

using integration by parts and recurrence relations for Legendre functions.

- 
- [1] H. B. G. Casimir, *Proc. K. Ned. Akad. Wet.* **51**, 793 (1948).
  - [2] T. Emig, A. Hanke, R. Golestanian, and M. Kardar, *Phys. Rev. Lett.* **87**, 260402 (2001).
  - [3] O. Kenneth and I. Klich, *Phys. Rev. Lett.* **97**, 160401 (2006).
  - [4] R. Balian and B. Duplantier, *Ann. Phys. (NY)* **104**, 300 (1977).
  - [5] R. Balian and B. Duplantier, *Ann. Phys. (NY)* **112**, 165 (1978).
  - [6] M. G. Krein, *Mat. Sborn. (NS)* **33**, 597 (1953).
  - [7] M. G. Krein, *Sov. Math.-Dokl.* **3**, 707 (1962).
  - [8] M. S. Birman and M. G. Krein, *Sov. Math.-Dokl.* **3**, 740 (1962).
  - [9] J. Schwinger, *Lett. Math. Phys.* **1**, 43 (1975).
  - [10] D. Langbein, *Theory of Van der Waals Attraction* (Springer-Verlag, Berlin, 1974).
  - [11] E. I. Kats, *Sov. Phys. JETP* **46**, 109 (1977).
  - [12] M. T. Jaekel and S. Reynaud, *J. Phys. I* **1**, 1395 (1991).
  - [13] A. Lambrecht, P. A. Maia Neto, and S. Reynaud, *New J. Phys.* **8**, 243 (2006).
  - [14] M. Henseler, A. Wirzba, and T. Guhr, *Ann. Phys. (NY)* **258**, 286 (1997).
  - [15] A. Wirzba, *Phys. Rep.* **309**, 1 (1999).
  - [16] A. Bulgac and A. Wirzba, *Phys. Rev. Lett.* **87**, 120404 (2001).
  - [17] A. Bulgac, P. Magierski, and A. Wirzba, *Phys. Rev. D* **73**, 025007 (2006).
  - [18] A. Wirzba, *J. Phys. A* **41**, 164003 (2008).
  - [19] T. Emig, N. Graham, R. L. Jaffe, and M. Kardar, *Phys. Rev. Lett.* **99**, 170403 (2007).
  - [20] O. Kenneth and I. Klich, *Phys. Rev. B* **78**, 014103 (2008).
  - [21] S. J. Rahi, T. Emig, N. Graham, R. L. Jaffe, and M. Kardar, *Phys. Rev. D* **80**, 085021 (2009).
  - [22] H. Gies and K. Klingmüller, *Phys. Rev. Lett.* **97**, 220405 (2006).
  - [23] A. Weber and H. Gies, *Phys. Rev. D* **80**, 065033 (2009).
  - [24] M. F. Maghrebi, S. J. Rahi, T. Emig, N. Graham, R. L. Jaffe, and M. Kardar, *Proc. Natl. Acad. Sci. USA* **108**, 6867 (2011).
  - [25] N. Graham, A. Shpunt, T. Emig, S. J. Rahi, R. L. Jaffe, and M. Kardar, *Phys. Rev. D* **81**, 061701 (2010).
  - [26] N. Graham, A. Shpunt, T. Emig, S. J. Rahi, R. L. Jaffe, and M. Kardar, *Phys. Rev. D* **83**, 125007 (2011).
  - [27] D. Kabat, D. Karabali, and V. P. Nair, *Phys. Rev. D* **81**, 125013 (2010).
  - [28] D. Kabat, D. Karabali, and V. P. Nair, *Phys. Rev. D* **82**, 025014 (2010).
  - [29] N. Graham, *Phys. Rev. D* **87**, 105004 (2013).
  - [30] E. N. Blose, B. Ghimire, N. Graham, and J. Stratton-Smith, *Phys. Rev. A* **91**, 012501 (2015).
  - [31] K. A. Milton and J. Wagner, *J. Phys. A* **41**, 155402 (2008).
  - [32] M. T. H. Reid, A. W. Rodriguez, J. White, and S. G. Johnson, *Phys. Rev. Lett.* **103**, 040401 (2009).
  - [33] Edited by D. Dalvit, P. Milonni, D. Roberts, and F. da Rosa, *Geometry and Material Effects in Casimir Physics-Scattering Theory* (Springer-Verlag, Berlin, 2011), pp. 129–174.

- [34] C.-T. Tai, *Dyadic Green Functions in Electromagnetic Theory* (IEEE Press, New York, 1994).
- [35] T. Emig, N. Graham, R. L. Jaffe, and M. Kardar, *Phys. Rev. A* **79**, 054901 (2009).
- [36] J. Meixner, *Z. Naturforsch.* **3a**, 506 (1948).
- [37] J. W. Meixner and R. W. Schäfke, *Mathieusche Funktionen und Sphäroidfunktionen* (Springer-Verlag, Berlin, 1954).
- [38] C. Flammer, *Spheroidal Wave Functions* (Stanford University Press, Stanford, CA, 1957).
- [39] T. Emig, *J. Stat. Mech.* (2008) P04007.
- [40] P. A. Maia Neto, A. Lambrecht, and S. Reynaud, *Phys. Rev. A* **78**, 012115 (2008).
- [41] N. Graham and K. D. Olum, *Phys. Rev. D* **72**, 025013 (2005).
- [42] P. E. Falloon, P. C. Abbott, and J. B. Wang, *J. Phys. A* **36**, 5477 (2003).
- [43] D. Varshalovich, A. Moskalev, and V. Khersonsky, *Quantum Theory of Angular Momentum: Irreducible Tensors, Spherical Harmonics, Vector Coupling Coefficients, 3-j Symbols* (World Scientific, Hackensack, NJ, 1988).
- [44] A. Forrow and N. Graham, *Phys. Rev. A* **86**, 062715 (2012).
- [45] R. Friedberg, *Am. J. Phys.* **61**, 1084 (1993).
- [46] C. D. Fosco, F. C. Lombardo, and F. D. Mazzitelli, *Phys. Rev. D* **84**, 105031 (2011).
- [47] G. Bimonte, T. Emig, R. L. Jaffe, and M. Kardar, *Europhys. Lett.* **97**, 50001 (2012).
- [48] A. Erdélyi, W. Magnus, F. Oberhettinger, and F. G. Tricomi, *Higher Transcendental Functions* (McGraw-Hill, New York, 1953).
- [49] M. Abramowitz and I. A. Stegun, *Handbook of Mathematical Functions with Formulas, Graphs, and Mathematical Tables* (U.S. Government Printing Office, Washington, DC, 1972).
- [50] I. S. Gradshteyn and I. M. Ryzhik, *Table of Integrals, Series, and Products*, 5th ed. (Academic Press, San Diego, 1994).